Local structures in medium-sized Lennard-Jones clusters: Monte Carlo simulations

W. Polak
Department of Applied Physics, Institute of Physics, Technical University of Lublin, ul. Nadbystrzycka 38, 20-618 Lublin, Poland

A. Patrykiejew
Department for the Modelling of Physico-Chemical Processes, Maria Curie-Skłodowska University, 20-031 Lublin, Poland
(Received 3 July 2002; revised manuscript received 27 December 2002; published 6 March 2003)

The Lennard-Jones clusters composed of approximately 200 atoms were simulated using canonical Monte Carlo method at the reduced temperatures between $T^*=0.05$ and $T^*=0.49$. Local arrangements of atoms within the clusters were identified by means of a specially invented algorithm based on the classification of five types of regular coordination polyhedra corresponding to face-centered cubic (fcc), hexagonal close-packed (hcp), icosahedral (ic), pentagonal direct-packed (pdp), and body-centered cubic (bcc) local structures. Clusters cut off from three types (fcc, hcp, and bcc) of perfect crystals show a structural transition with gradually increasing temperature in the temperature range corresponding to solid clusters. The spectrum of 201 atomic clusters formed at the temperature $T^*=0.25$ from a starting configuration with random atom positions is characterized by a variety of local structures, with quantitative dominance of hcp and pdp structural units and absence of bcc units. Most of these clusters are polyicosahedral, very often showing a triangular or tetrahedral arrangement of ic units. In some clusters noncrystallographic ic and pdp atom arrangement is absent. In such cases spatial separation of two crystallographic phases can be observed in the form of fcc and hcp domains or as sandwiched parallel fcc and hcp planes.

DOI: 10.1103/PhysRevB.67.115402 PACS number(s): 64.70.Nd, 02.70.Uu, 36.40.Ei, 65.80.+n

I. INTRODUCTION

Experiments show that bulk crystals of rare gases, except helium, adopt the face-centered cubic (fcc) structure.[1] However, calculations of lattice energy indicate that the hexagonal close-packed (hcp) structure is energetically slightly more stable, independently of the form of the pair-potential applied (for details, see Refs. 2,3, and the literature cited therein). In spite of the many attempts discussed e.g., in Refs. 3–5, this *rare gas solid problem* (RGS problem) has not yet been satisfactorily explained. In order to find the solution to the RGS problem, many authors have concentrated on the analysis of the structure of finite clusters formed during early stages of the homogenous nucleation process.

Homogeneous nucleation of a rare gas can be experimentally studied by supersonic expansion of a gas through a nozzle into vacuum.[6,7] Cluster beams formed during the vapor condensation process are then typically investigated using mass spectrometry. Analysis of the experimental data on the cluster abundance reveals the existence of *magic numbers* in the cluster spectrum. Some of the peaks are identified to correspond to closed shell icosahedral forms,[6,7] while the others can be qualitatively interpreted assuming the growth scheme based on the formation of the next shell of icosahedron due to the decoration of the core (closed shell) by atoms at sites of high symmetry.[6] However, these results partly contradict those obtained from the analysis of electron diffraction data.

Starting from the early experiments of Farges *et al.*,[8] a vast body of experimental results for noble gas clusters of different size have been collected. Unfortunately, the diffraction patterns are rather difficult to interpret. It was pointed out by van de Waal *et al.*[5] that the observed diffraction patterns unavoidably represent the averages over many clusters, which, most likely, have different size and structure. Moreover, it is extremely difficult to determine a ''true atom arrangement'' in a cluster of a given size. For example, Farges *et al.*[8] interpreted the diffraction pattern obtained for argon clusters and suggested that the clusters contain about 500 atoms and possess the fcc structure built upon noncrystalline nuclei. The same pattern was then reinterpreted by van de Waal.[9] He concluded that it corresponds to a considerably larger cluster of about 3000 atoms and of multiply twinned core of fivefold uniaxial symmetry which enables overgrowth of the fcc structure. It has been clearly shown[9] that the diffraction pattern cannot be explained assuming a single ''pure'' fcc, hcp, multishell Marks decahedron as well as a multishell icosahedral (MIC) cluster structure.

Recent experiments[5,10,11] with supersonic cluster beams reveal a complex structure in large noble gas clusters due to detection of stacking faults or twinning faults and deformations as well as the coexistence of fcc and hcp phases. Kovalenko *et al.*[10] reported a defective fcc structure in rare gas clusters of sizes $N \geqslant 1500$ in the form of small hcp interstitial in the fcc structure. Feraudy and Torchet[11] found signs of hexagonal symmetry in clusters and twin faults in fcc stacking. According to van de Waal *et al.*,[5] large argon clusters of $10^3 \leqslant N \leqslant 10^5$ have very complicated structure built probably from many twinned domains of fcc and hcp character.

Theoretical studies and computer simulations based on both Monte Carlo (MC) and Molecular Dynamics (MD) methods have often been used to investigate the structure of clusters and to determine the global minimum of the cluster binding energy. In such studies, one usually assumes that the atoms interact via pairwise additive central forces, most commonly described by the standard Lennard-Jones (LJ) potential. A numerical optimization method was used in the pioneering work of Hoare and Pal[12] to find a global mini-

 ©2003 The American Physical Society

mum of the potential energy of small clusters with the number of atoms up to ≈ 60. Then, it appeared that the solution of the RGS problem is getting even more complicated because the clusters corresponding to global minima often show noncrystalline icosahedral arrangement of atoms. While using this method one also encounters a purely technical, yet important, problem connected with the range of potential used in computation, since different potential ranges lead to geometrically different clusters which correspond to the global energy minimum.[13] Many problems in predicting cluster structure have their origin not only in the uncertainty of finding a global energy minimum but mainly in the assumption of zero temperature of a cluster. The optimal cluster structure at finite temperatures corresponds to the lowest Helmholtz free energy F. As found by Doye and Calvo,[14] the cluster temperature can be a key variable in determining the equilibrium structure of a cluster. However, those entropic and temperature effects are relatively rarely analyzed.[14–16]

MC and MD simulations allow for a more realistic analysis of clusters and of clustering processes since temperature is one of the simulation parameters. Entropy is also included in MC method by averaging over a great number of microstates accepted at a given temperature or present in the time evolution of the atomic system, governed by equations of motion used in MD. However, realistic simulations[17] of clustering during supersonic expansion are difficult. After having analyzed their MD simulation data, Ikeshoji *et al.*[17] found that introduction of cluster–cluster and cluster–atom collisions alone, with a linear decrease in temperature, does not lead to *magic numbers* found in the experimental data. They showed that evaporation must also be introduced in MD simulation in order to obtain results with cluster spectra similar to those observed in experiments. It was found[17] that clusters with the number of atoms close to magic numbers show a structure similar to that of polyicosahedral (first reported in Ref. 18) and MIC clusters, but clusters with $30 \leqslant N \leqslant 50$ are more amorphous or are mixtures of different series of structures. The existence of fcc structure with many defects is possible as well. In the relatively small Lennard-Jones clusters composed of 38 atoms simulated over a wide range of temperatures, Neirotti *et al.*[19] revealed the existence of fcc and ic structures, which transform one into another in the course of simulation.

Equilibrium behavior of LJ clusters at a given T can be more conveniently studied with the help of Monte Carlo simulations. Medium-sized LJ clusters were studied by Quirke,[20] who investigated melting transition and local arrangement of atoms using MC simulations. Clusters of the size $N=201$ and 209 were formed by placing all atoms in a spherical cavity and then by equilibrating the system at a given temperature. The local arrangement of atoms in the cluster core was then found by means of analysis of the cosine distribution curves of interior angles between triplets of atoms. Such calculations allow to obtain general information about the changes in the internal structure of the cluster, which occur during the freezing transition from the ic structure in liquid state to the dominating hcp structure with dislocations in solid state. Some dislocations were interpreted as the presence of a fcc local ordering around an atom.[20]

As a summary of the above cited literature, there are reports that cluster structure is highly symmetric, and corresponds to multishell icosahedra or decahedra as well as to pure fcc or hcp structures. Other results demonstrate the presence of more complex structures in the form of a mixture of different structures, defects and imperfections. Arguing that transformation between optimal structures is more difficult for large clusters,[14] and quite unlikely for the cluster sizes of 10^3–10^4 atoms,[21,22] the role of kinetics in the cluster growth have also been pointed out in the literature. Using MD simulations, Balletto *et al.* found that effects of kinetic trapping completely dominate the growth of C_{60} clusters,[23] and that the formation of large metastable silver icosahedra can be explained by kinetic factors.[24] Also, it is reasonable to expect that the flat faces of the clusters having an ideal structure should exhibit rather low growth rate. van de Waal suggested[9,21] in 1996 that the transition from ic to fcc structure can be triggered by the formation of linear defects with uniaxial pentagonal symmetry, which appear inside a cluster.

In our opinion, a detailed analysis of the internal structure of imperfect clusters (omitted in a vast majority of theoretical works) can lead to a better understanding of the formation of the fcc structure during a homogeneous cluster growth. It should be noted that the situation here is similar to that of the history of the study of the role of dislocations in a high growth rate of crystals, when all models based on the concept of a perfect crystal structure failed. It is one of the goals of our study to analyze local atom arrangement in simulated clusters formed and equilibrated at temperatures close to those used in experiments and to investigate the mechanisms of the fcc structure formation. Our analysis is not focused on finding the global minimum of the cluster potential energy but rather on obtaining stable (i.e., sufficiently well equilibrated) clusters to attain stable thermodynamic parameters. Local ordering of atoms in all such clusters is analyzed, mainly to find a cluster structure which promises the overgrowth of fcc structure.

Medium-sized LJ clusters built of a few hundreds of atoms seem to be an interesting case for investigation because they form a bridge between small clusters of noncrystalline (icosahedral, polyicosahedral or decahedral) character and large clusters, probably dominated by a mixture of the fcc and hcp structures. It is also worthwhile to analyze solid clusters which contain approximately 200 atoms because, as already mentioned, at least two types of local order, i.e., hcp and fcc, can appear.[20] Moreover, Kakar *et al.*[22] concluded from experimental data that a transition from the ic to the fcc structure in clusters of $N \geqslant 200$ may occur. In order to observe possible initial stages of that transition in medium size clusters as well as the coexistence of different types of local structure, a new algorithm for a precise determination of local structures is proposed. The algorithm is sensitive to the fcc, hcp, bcc, ic as well as to the decahedral local structures. Then spatial locations of different local structures and their changes as a function of temperature are analyzed for the clusters formed during the simulation.

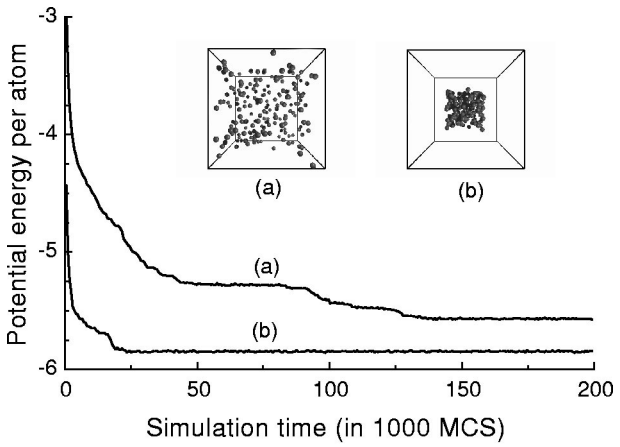

FIG. 1. Potential energy per atom in a cluster as a function of Monte Carlo steps. Two simulation processes differ only by the initial positions of atoms (illustrated in insets) randomly located: (a) in the entire simulation box, (b) in the central part of the box.

II. CLUSTER FORMATION METHOD

The formation of Lennard-Jones clusters was simulated by means of canonical Monte Carlo method. The Lennard-Jones potential,

$$U(r)=4\varepsilon\left[\left(\frac{\sigma}{r}\right)^{12}-\left(\frac{\sigma}{r}\right)^{6}\right], \tag{1}$$

was truncated at the distance $r_{\mathrm{cut}}=3.4\sigma$. Throughout this paper we use σ and ε as the units of length and energy, respectively. In particular, the reduced temperature, T^*, is defined as $T^*=k_BT/\varepsilon$, where k_B is the Boltzmann constant.

Periodic boundary conditions were implemented by replicating the cubic cell of edge length L, in a similar manner as done by Rytkönen *et al.*[25] in their study of argon clusters. It enables us to avoid problems encountered when atoms are placed in a spherical cavity used, for example, in papers:[20,26] no potential wall is needed, cluster can freely expand when heated, shape of the cluster is not influenced by the geometry of the wall, evaporation and attachment of atoms is enabled in the canonical ensemble.

MC simulations can be carried out for the starting configuration of a cluster with the number of atoms N and with predetermined structure and shape, e.g., a cluster of pure fcc structure and the shape in the form of truncated octahedron. Another case corresponds to a situation in which a cluster is formed during equilibration from a given number of atoms N placed at randomly chosen positions in the central cubic part of the simulation cell of edge length $L'<L$. At low temperatures, when the solid or liquid clusters rather than a gas phase are formed, this choice of starting configuration proved to be more efficient in attaining the equilibrium in the system more quickly than using the configuration with atoms placed in the entire box (see Fig. 1). It happens due to a substantial reduction in the random-walk like behavior of atoms. The optimal value of the edge length L' of the initial box was estimated by a trial and error method to be close to $1.5N^{1/3}$, which gives significantly lower atom density than that obtained in the final clusters. This trick successfully eliminates a time consuming Oswald ripening period (reported for 2D case by Mahnke *et al.*)[27] and avoids the formation of many isolated clusters.

Our algorithm is based on the standard Metropolis sampling method and involves the displacement of a randomly selected atom by a randomly chosen vector within a cube of the edge length $2\Delta r_a$, where Δr_a is the maximum allowed displacement in one direction. Each Monte Carlo step (MCS) involved N attempts to displace a randomly selected atom. The value of the maximum allowed displacement was adjusted during the simulation in order to keep the acceptance ratio close to 0.4.

A pair of atoms i and j, separated by a distance r_{ij}, lower than a certain predefined distance $r_{\mathrm{cl}_{\mathrm{cut}}}$, are assumed to be sufficiently strongly bound to the same cluster. The cluster identification procedure was invoked every 10th MCS. Whenever the number of clusters $N_{\mathrm{cl}}\geqslant 2$, the random moves of also randomly selected clusters were performed with the maximum displacement Δr_{cl} of the cluster mass center (in three directions X, Y, and Z). After such a movement, the resulting energy difference was computed for the entire system and the movement was accepted or rejected in accordance with the Metropolis criterion. Moreover, rotations of clusters around 3 axes coming through the cluster mass center were applied. The displaced or rotated clusters are able to consume isolated atoms or to join other clusters. The latter process significantly decreases the time necessary for attaining the equilibrium in the system, but only at sufficiently high temperature and when the number of vapor atoms is not equal to zero.

A given number of Monte Carlo steps $\mathrm{MCS}_{\mathrm{eq}}$ was used to equilibrate the system. The changes of the potential energy per atom, U/N, were monitored to find whether the system had reached a steady state (see Fig. 1). Then, during the averaging period, the parameters of the entire system, like the radial distribution function $g(r)$, the number of identified units N_{str} of analyzed local structures (method presented in the next section) and the specific heat C_V, were calculated. The latter parameter was obtained from the fluctuation theorem

$$C_V=\langle U^2-\langle U\rangle^2\rangle/(NT^2). \tag{2}$$

III. ARRANGEMENT OF ATOMS IN CLUSTERS OF SPECIFIC GEOMETRY

There are several methods which allow to identify local ordering of atoms in 3D systems. One of them is the analysis of cosine distributions of interior angles between triplets of atoms.[20] The peaks corresponding to the perfect hcp and icosahedral (ic) local structures are located at different sets of cosine values: $(-1,-0.83,\pm 0.5,-0.33,0.0)$ and $(-1,\pm 0.5)$, respectively. The method, however, may give incorrect results when applied to local environment of a chosen atom at a given moment of simulation. It happens due to several reasons: (i) similarity of cosine distributions for fcc and hcp local structures, (ii) large distortions of local structures in a cluster, and (iii) lack of averaging over many succeeding configurations. Note that both the fcc and hcp struc-

tures give peaks at $(-1, \pm 0.5, 0.0)$. Therefore, the method is not always reliable and it may happen that a small number of atoms being a part of the local fcc structure are overlooked. Only visual inspection of atomic layers[20] and calculation of the triplet cosine distribution for a chosen atom can reveal the local fcc structure around the atom.

The second method is the SO(3) invariant analysis based on the use of the spherical harmonics and two angles expressing bond orientation as proposed by Steinhardt *et al.*[28] and developed or modified by different authors.[19,29–31] It allows us to identify crystalline and icosahedral structures. It happens, however, that using this method it is difficult to distinguish between different cluster structures and additional tests like quenching of selected structures must be applied.[19] As proved by the authors of this work, probably this is due to the fact that some structural parameters, mainly Q_4, are higly sensitive to even slight distortion of local structures present, for example, in MIC clusters (see Table II).

The third method[32,33] is based on the construction of the Voronoi polyhedra (VP) around each atom and subsequent classification of their shapes by comparing geometrical parameters with predefined patterns describing the VP of different ideal crystal structures. However, before comparison, special attention must be paid to the elimination of VP small faces and short edges formed due to thermal displacement of atoms in the system. This has been realized[32,33] by an additional algorithm using arbitrary, although optimized, pair of parameters.

It is typical for all methods based on the comparison with sets of patterns that none allows the identification of the local structures of an unexpected regular form as the unknown structure has not been parametrized before. It certainly remains true for the three methods described above.

In the beginning of our analysis, the unique reliable method to not omit any possible types of regular local order in the system, was a visual inspection of a large number of local configurations of atoms. Although it is a tedious and time consuming task, it can be quite efficiently used with the help of available software, such as the MSI Visualizer, which allows us to look easily at the local configuration of atoms. In order to prepare the files in the MSI format an additional program was used. It was based on: (a) finding all atoms with 12 first nearest neighbors in the sphere of radius R_n, built around a central atom, and (b) connecting by a line the ith and jth neighboring (vs central one) atoms when the distance r_{ij} between them is less than the allowed maximum distance $D_{\max}$. The parameter $D_{\max}$ was chosen to be equal to 1.35, according to the data from[20] used for cosine analysis. This value corresponds approximately to the upper limit of the radius of the first coordination shell in solid clusters.

Coordination polyhedra obtained as described above have the shape of cubo-octahedron (COCT), anti-cubo-octahedron (ACOCT), and icosahedron (IC) for, respectively, fcc, hcp, and ic structure (see Fig. 2). Careful examination of all polyhedra built of 12 atoms enabled us to discover one more regular structure in the form of the truncated decahedron (TDH) shown in Fig. 2(d). This local structure has uniaxial pentagonal symmetry with atoms arranged along this axis and is named hereafter as ''pentagonal direct-packed (pdp).''

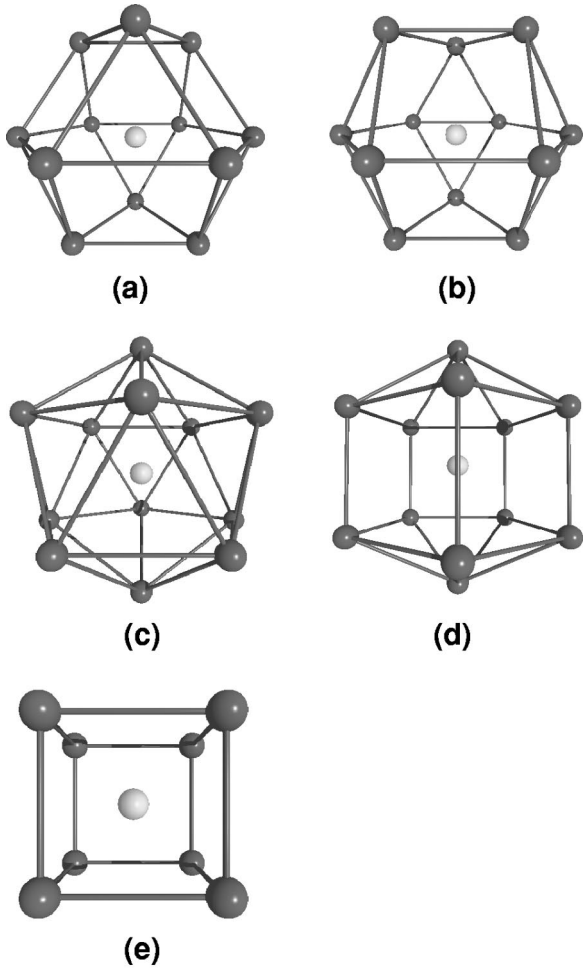

FIG. 2. Coordination polyhedra representing five investigated local structures: (a) cubo-octahedron (fcc), (b) anti-cubo-octahedron (hcp), (c) icosahedron (ic), (d) truncated decahedron (pdp), and (e) cube (bcc).

Analysis of the geometry of pdp local structure reveals that each pdp unit can be treated as composed of two pentagonal dodecahedra having a common vertex atom as well as a common fivefold symmetry axis. The formation of practically the same atom arrangement during the growth of small pentagonal decahedron particles was postulated in 1969 by Fukano and Wayman.[34]

As mentioned already, visual inspection of a large number of coordination polyhedra is rather tedious and time consuming. Therefore, it was necessary to apply an algorithm for the automatic identification of the shape of four polyhedra mentioned above. We also decided to add the possibility of recognizing the bulk centered cubic (bcc) structural unit, represented by the coordination polyhedron in the form of cube [Fig. 2(e)]. The algorithm is based on counting the number of (a) edges at each of the 12 or 8 vertices, (b) triangular faces, and (c) the neighborhood-type of triangular faces (number of edge and vertex contacts), and assumes the following geometrical criterion for atom packing: $D_{\max}=R_n$, with the exception of the bcc structure where $D_{\max}=2R_n/\sqrt{3}$ is taken. All these parameters are presented in Table I. A specially written computer program was tested to give 100% accurate

TABLE I. Number of vertex edges, triangular faces, and their neighborhood types for all analyzed coordination polyhedra: cubo-octahedron, anti-cubo-octahedron, icosahedron, truncated decahedron, and cube, representing five types of local structures. Abbreviations used in the last column e.g. for IC "20 × (3 e, 6 v)" denote that each of the 20 triangular faces in the icosahedron has the contact with three neighboring triangular faces by edge, and with six neighboring triangular faces by vertex.

Polyhedron	Structure	Vertex edges	Triangular faces	Neighborhood type
COCT	fcc	12 × 4	8	8 × (0 e, 3 v)
ACOCT	hcp	12 × 4	8	6 × (1 e, 1 v)
				2 × (0 e, 3 v)
IC	ic	12 × 5	20	20 × (3 e, 6 v)
TDH	pdp	10 × 4	10	10 × (2 e, 2 v)
		2 × 5		
Cube	bcc	8 × 3	0	

results when applied to clusters with a total number of ≈ 1000 different local structures, which have been visually inspected before. However, a more detailed analysis of the structures in systems at different temperatures revealed that any rigidly selected value of $D_{\max}$ and R_n may result in the omission of some coordination polyhedra (structural units). Therefore, during one run of the program many attempts had to be made with increasing value of R_n. It turned out that optimal values are: the lower limit of $R_n = 1.05$, the upper limit $R_n = 1.55$, and $\Delta R_n = 0.01$ for the radius increment.

A special program, which enables to prepare input files for a visualizer or a 3D graphics program, like POVRAY (used by the authors of this work), has proved to be very useful. The presentation of the selected local structure in most figures in this work has been done as follows: (a) the position of centers of the local structure are shown by light gray balls, (b) all neighboring atoms/balls, which are centers of the given local structure, are connected by thick dark lines if their separation is not larger than $R_n = 1.35$, (c) positions and bonds of surface atoms are marked only by thin gray lines, and (d) all remaining bonds inside the cluster were omitted to make the presentation clear. However, in case of two of the figures, connections between neighboring atoms (vs local structure center) are also shown by thick dark lines in order to better illustrate cluster geometrical properties.

As an example, the coordination polyhedron method (CP method) is applied to analyze and visualize internal structure in ideal multishell icosahedral clusters. Sufficiently large (starting from 309 atoms) MIC clusters contain 4 types of local order [see Fig. 3(b)]: one ic unit in the cluster center, 12 linear pdp chains each connecting the cluster center with a cluster vertex, and numerous hcp local structure in the entire cluster volume mixed with the fcc structure. The fcc structure is absent in small MIC clusters composed of 55 or 147 atoms, as shown in Fig. 3(a). The above figures may be useful for those, who are searching for an ideal ic structure in medium or large clusters with the number of atoms different from an ideal MIC cluster. Characteristic 6 linear pdp chains coming through one ic unit can serve as a fingerprint of such clusters.

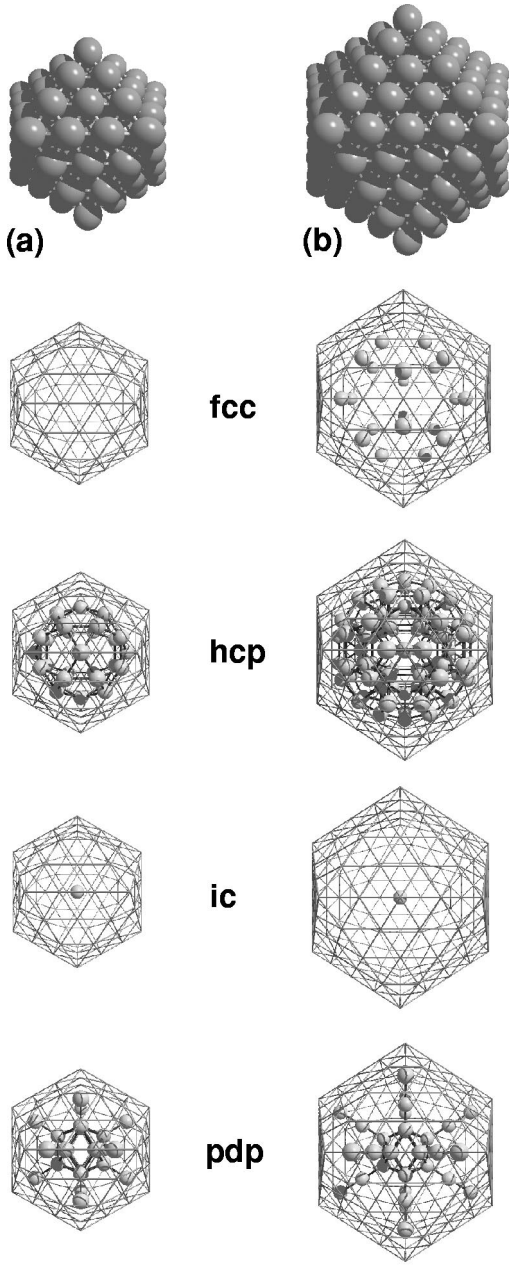

FIG. 3. Atom configuration in multishell icosahedral clusters composed of (a) 147, (b) 309 atoms. Atoms and bonds belonging to all detected local structures in the clusters are shown in the lower part of the figure.

The detected local structures were characterized using the method of calculations of the order parameters Q_4 and Q_6 given by Doye *et al.*[31] In order to characterize a local structure, the averaging over bonds was always limited to twelve vectors connecting the central atom of the local structure and a neighboring atom. The values of the parameters are compared in Table II with those obtained for local structures in ideal clusters. The ideal clusters are a piece of ideal crystal structure (fcc or hcp) as well as optimised LJ_{13} of ic or pdp atom arrangement. It is evident from Table II that the param-

TABLE II. Values of order parameters Q_4 and Q_6 calculated for the local structures present in multishell icosahedral (MIC) clusters compared with the values for undistorted local structure in monostructural ideal clusters.

Type of local structure	Monostructural ideal cluster		MIC cluster	
	Q_4	Q_6	Q_4	Q_6
fcc	0.191	0.575	0.196	0.569
hcp	0.097	0.485	0.117	0.481
ic	0.000	0.663	0.000	0.663
pdp	0.076	0.435	0.053	0.430

TABLE III. Binding energy (potential energy per atom) of ideal infinite crystal structure optimized with respect to the atom separation distance for the force cutoff $r_{cut}=3.4$. Columns 4 and 5 give numbers of atoms and energies at $T^*=0$ of initial quasispherical clusters, which have been used in our calculations.

Structure	Infinite structure		Spherical cluster	
	Interatomic distance	Binding energy	Number of atoms	Binding energy
bcc	1.0713	−8.0077	181	−5.6271
fcc	1.0927	−8.3766	201	−6.0784
hcp	1.0903	−8.3830	195	−5.9788

eters Q_4, with the exception of ic, are significantly different. This may be attributed to a distortion of local structures present in MIC clusters.

IV. RESULTS

All simulations were carried out for the potential cutoff set at $r_{cut}=3.4$, following the data of Ref. 25. In order to obtain an isolated cluster, i.e., the one that does not interact with its replicas in neighboring cells, we decided to choose a sufficiently large cell of the edge length $L=20$. However, it should be noted that this procedure does not rule out interactions between different clusters, if they are spontaneously formed during the simulations. Our cluster identification procedure is based on the measurements of interatomic distances between neighbors. For a given pair of atoms, if this distance is smaller than $r_{cl_{cut}}=1.5$ (cf. Ref. 35), the atoms are recognized to be a part of the same cluster.

As mentioned in Sec. II, whenever the number of clusters $N_{cl}\geqslant 2$, N_{cl} translation and rotation moves of clusters have been performed every 10th MC step. Each translation and rotation move has been applied to randomly selected clusters (chosen with equal probability). Since evaporation of the main cluster composed of approximately 200 atoms is observable in our simulations practically only when the cluster is in a liquid state, the cluster translations and rotations can then be applied. Their impact on the system properties is observable only in the simulations of clusters heated to temperatures above the melting point. In cluster translations $\Delta r_{cl}=3.0$ was used, which is relative large in comparison with a typical value of the maximum allowed atom translation $\Delta r_a \in (0.05, 0.25)$ (depending on the system temperature). The maximum rotation angle was fitted to 180°, which enabled total rotation of the cluster. Due to relatively low number of vapor atoms, reaching hardly 2–4 atoms at the maximum analyzed temperature of $T^*=0.49$, the acceptance ratio of cluster movements was high and the additional adjusting of these parameters was not possible.

Finally, it is worth mentioning that the bcc structural units were not detected in any of the final clusters. During a cluster simulation connected with ≈20 000 of attempts of the local structure identifications in entire cluster, only a few to a few tens of bcc structural units were recorded, mainly when the cluster temperature was close to the cluster melting temperature. Therefore, more detailed examination of the bcc structure was excluded from our analysis.

A. Heating up the perfect clusters

Comparison of our cluster energies needs a reference point, which should be a cluster with the highest binding energy. There are suggestions in the literature[13] that an optimal (most strongly bonded) cluster of $N=201$ atoms corresponds to the form of truncated octahedron with the fcc packing. Such clusters are obtained by cutting a piece of fcc infinite ideal structure by a sphere. It is resonable to expect also high, if not higher, binding energy for clusters with icosahedral atom arrangement. A cluster of this type can be built by removing some atoms on the external facets of the 309-atom multishell icosahedron reaching the size 201. As proven in this work for $T^*=0.05$, the fcc cluster really has a sligthly higher value of the binding energy (i.e., −6.016) than the incomplete MIC cluster (−6.015). Therefore, we decided to choose the fcc cluster as the reference point at all analyzed temperatures, knowing, however, that entropy contribution can be decisive at this cluster size.

In order to compare and improve the understanding of simulation results, a similar procedure of comparision of binding energy was also undertaken using the spherical hcp cluster with 195 atoms and bcc cluster with 181 atoms. Atom separation in each of the above mentioned infinite ideal structures was optimized for the value of force cutoff used in this particular case to obtain the maximum value of crystal binding energy per atom. As shown in Table III, the magnitude of the cluster binding energy per atom is always significantly smaller than that of the infinite crystal due to the existence of cluster surface. Moreover, the hcp structure has a slightly higher binding energy than the fcc structure, and the bcc structure is a relatively weakly bonded crystal structure.

The stability of the initially perfect structure of all the three types of clusters was confirmed by MC simulations along the path of gradually increasing temperature. The heating up process was realized by (a) selecting a cluster, in its final configuration of atoms, at a given low temperature T^*, (b) increasing the simulation temperature by the increment $\Delta T^*=0.02$, (c) equilibrating the system at the temperature $T^*+\Delta T^*$, using at least 200 000 MC steps, and (d) calcula-

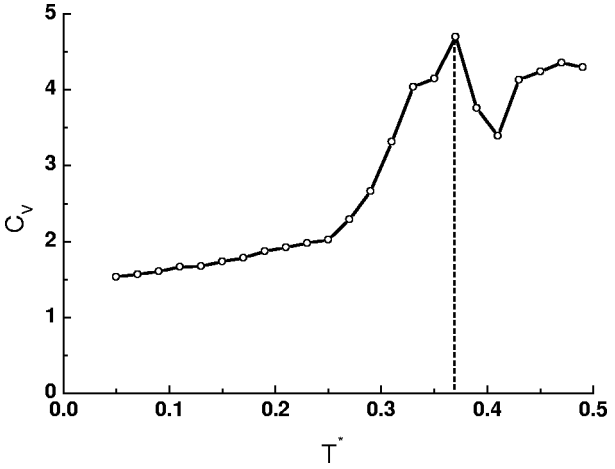

FIG. 4. Dependence of the specific heat C_V on the cluster temperature obtained during the heating up of the fcc cluster. The peak on the curve, pointed out by a dashed line, corresponds to the cluster melting temperature.

tion of all quantities of interest, averaged over the subsequent 200 000 Monte Carlo steps. Such simulations were carried out 17 times for the ideal fcc cluster, each starting with a different seed of the random number generator. For the sake of comparison, 10 simulations for hcp and one for bcc initial clusters were also done. The cluster annealing process was monitored by the calculation of specific heat C_V, which reveals the point of a solid–liquid transition in the cluster, manifested by the appearance of a maximum (see Fig. 4). The average melting temperature T_m^* for the fcc cluster was estimated to be $T_m^* = 0.37$. This value agrees very well with the results of Quirke,[20] who also studied clusters composed of $N = 201$ atoms. The decrease in the absolute values of the cluster binding energy per atom (Fig. 5) during the temperature increase is caused by larger thermal displacements of atoms at higher temperatures. This also leads to a considerable increase in the value of the standard deviation of binding energy as is also illustrated in Fig. 5 for the fcc cluster.

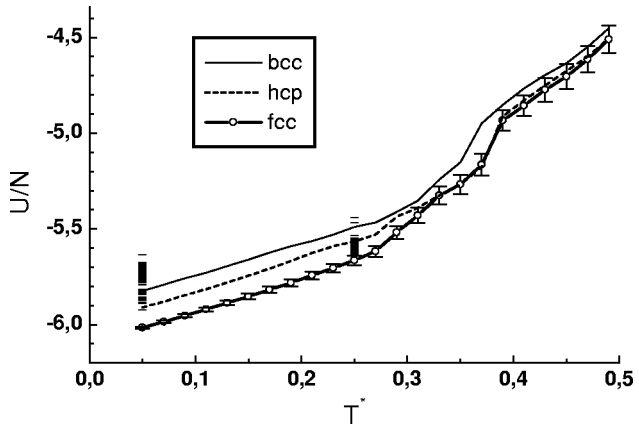

FIG. 5. Potential energy per atom during the heating up of three types of spherical clusters with initial (at $T^* = 0$) structure: bcc ($N = 181$), hcp ($N = 195$), and fcc ($N = 201$). Potential energy levels of 80 clusters formed at $T^* = 0.05$ and 100 clusters at $T^* = 0.25$ are also shown as horizontal bars.

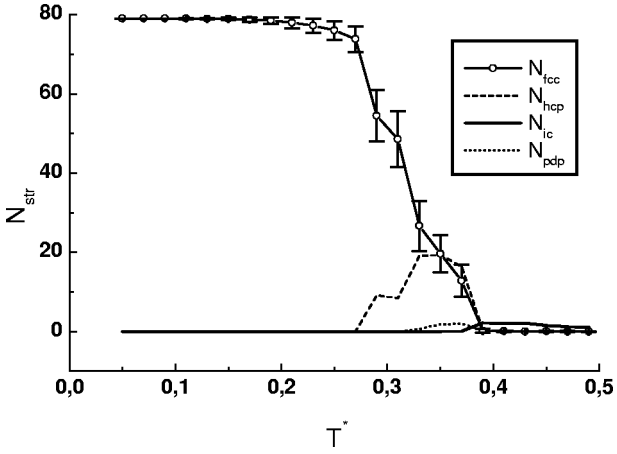

FIG. 6. The number of structural units of four types present in the initially perfect fcc cluster during their heating up from $T^* = 0.05$ to $T^* = 0.49$. The standard deviation is shown for the fcc local structure.

Due to the surface effect, smaller clusters with $N = 181$ and $N = 195$ are characterized by lower values of the binding energy.

Thermal atom displacements can also destroy or transform initial atom configuration. To observe and measure this effect, the internal structure during the heating up of clusters is analyzed using the coordination polyhedron method. It was observed that all bcc structure centers rapidly disappear during the first 1000 MCS of equilibration at $T^* = 0.05$, which was accompanied by the formation of 8 fcc and 53 hcp centers. Such atom rearrangement also occurs for the initially pure hcp cluster, yet at a significantly higher temperature, between $T^* = 0.21$ and $T^* = 0.25$, when the formation of many fcc units are observed.

All 17 simulations for the heating of the fcc cluster lead to the transformations of cluster internal structure. Without any exception, at $T^* \approx 0.29$, hcp structural units are formed and two types of phases: fcc and hcp, are observed to coexist. Typically, hcp structural units are created on the cluster surface and collected in 1–3 domains, sometimes in the form of a nice plane. In most cases, the formation of the pdp structure (generally at the cluster surface) was found to occur at slightly higher temperature ranging from $T^* = 0.31$ to 0.37 in different simulation runs. Finally, near the cluster melting point $T_m^* \approx 0.37$ the ic structure occurs. At higher temperatures when the liquidlike phase is formed, the clusters are characterized by the presence of 1–3 ic units, while fcc, hcp, and pdp structural units do not appear. These structural changes are illustrated in Fig. 6 for the heated fcc cluster. In Fig. 6, also one can see that the standard deviation of the number of fcc centers is very large during the phase transformation from fcc to hcp and then to pdp in the solid cluster (points on the slope of N_{fcc} plot).

Spatial location of all structures presented in one of the annealed fcc clusters is shown in Fig. 7 for four different temperatures. Before the structural transformation, at $T^* = 0.27$ practically all atoms belong to the fcc structure, while other local structures do not exist. Then at $T^* = 0.29$ the hcp centers on the cluster surface are created. After the further

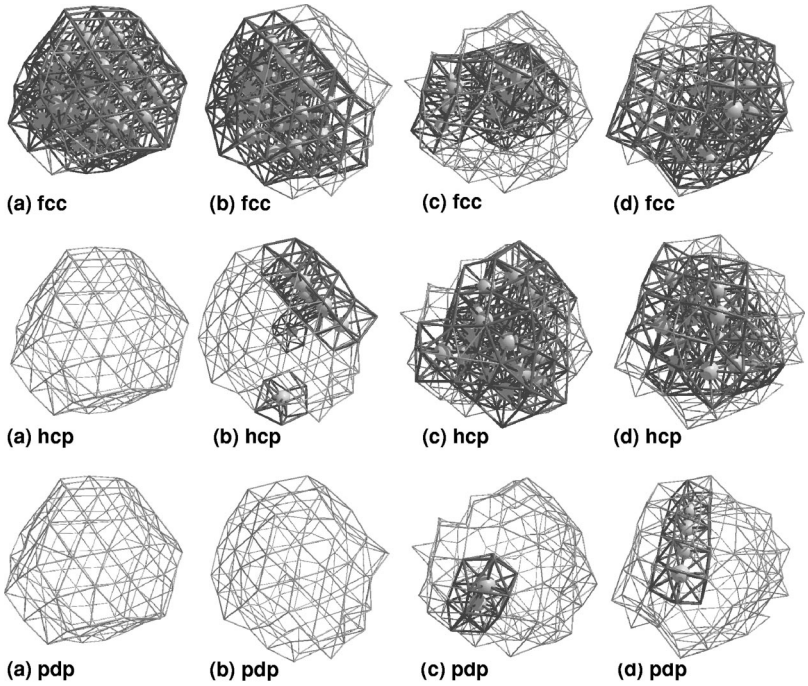

FIG. 7. Spatial location of all structures presented in the heated fcc cluster for four different temperatures: (a) $T^*=0.27$, (b) $T^*=0.29$, (c) $T^*=0.31$, and (d) $T^*=0.33$.

temperature increase, to $T^*=0.31$ hcp spreads over the entire cluster near its surface, while the fcc remains in the cluster core. Moreover, the pdp structure is created on the cluster surface in the form of two neighboring pdp centers. Figures 7(c) and 7(d) demonstrate an interesting phenomenon, where, contrary to the ideal multishell icosahedral clusters, pdp units can also exist in clusters when the ic structure is absent. Characteristic phase changes originating near the cluster surface have already been reported in the literature[26] for LJ clusters as surface melting occurring for $N\approx 30$, where solid cluster core and liquidlike surface coexist. Similar phenomenon, solid-to-solid transformation from fcc to ic structure was reported by Cleveland *et al.*[36] to be precursors to the melting transition in simulated gold clusters.

B. Clusters formed at constant temperature

In order to understand better the cluster structural properties at a given temperature, the simulations should involve formation and analysis of as many clusters as possible. However, the number of such clusters was limited in this work by the available time of computer processing, and then by the visual analysis of spatial location of the five possible types of local structures in each cluster. Therefore, we consider only the formation of clusters built of $N=201$ atoms, and the number of attempts of the cluster formation equals to 80 at $T^*=0.05$ and 100 at $T^*=0.25$. The equilibration process is sufficiently long (minimal number of MC steps is 700 000 for lower, and 300 000 for higher temperature) to obtain a well equilibrated cluster, as far as its energy, specific heat, and the number of structural units are concerned. Therefore, each of these clusters corresponds to a local minimum of the free energy. Although the method used here does not guarantee the global minimum to be reached, the authors have been very careful to avoid high lying local minima. This problem is very serious, especially at low temperatures. As shown in Fig. 5, the energy levels of all clusters at the low temperature of $T^*=0.05$ are far apart, while at $T^*=0.25$ the energy gap becomes very small and for some clusters the energy becomes very close to the energy of the fcc cluster. The above comparison of cluster energies and the arguments that cluster growth does not always lead to global minima to occur (see Introduction) allow us to infer that some of the clusters obtained here at $T^*=0.25$ can occur in real growth conditions.

Statistics of different structural units existing in clusters formed at both temperatures used here is compared in Fig. 8. It is clearly seen that at the higher temperature ($T^*=0.25$), the number of identified local structures: N_{fcc}, N_{hcp}, and N_{pdp}, enormously increases, while only N_{ic} slightly decreases. This means that the clusters at $T^*=0.25$ are ordered much better. To measure the ordering of cluster atoms, we introduce the cluster ordering parameter F_o defined as

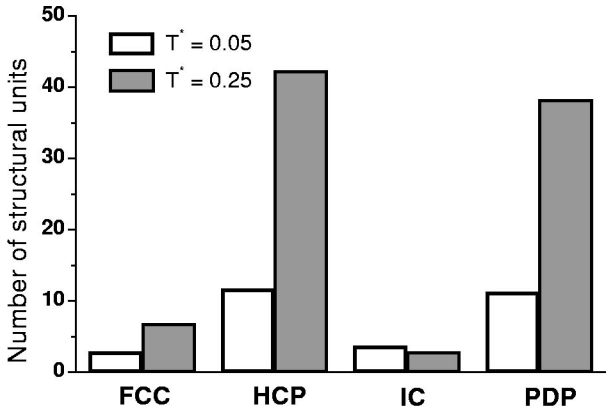

FIG. 8. Average number of structural units present in the final configuration of all clusters formed at two different temperatures: $T^*=0.05$ and $T^*=0.25$.

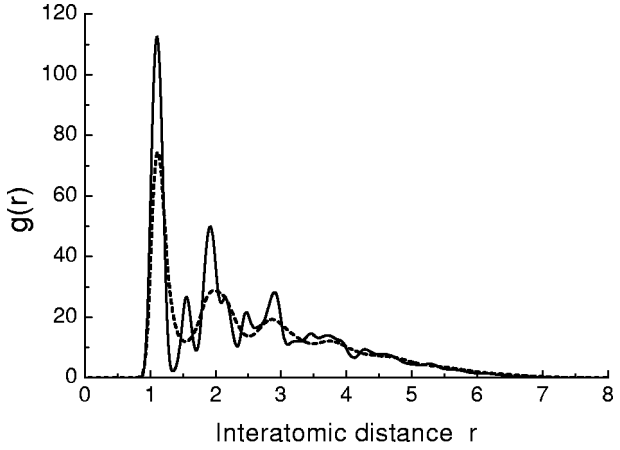

FIG. 9. Radial distribution function calculated for one of solid clusters formed at $T^*=0.25$. Dashed line corresponds to the rdf of the same melted cluster at $T^*=0.43$.

$$F_o = N_{\mathrm{ls}}/N_{12}, \tag{3}$$

where N_{ls} is the sum of all atoms which are centers of any of the five analyzed local structures, and N_{12} denotes the number of atoms in the cluster, which have 12 nearest neighbors with a distance not larger than $R_{12_{\max}}$. This latter parameter was set here to be equal to $R_{g_{\min 1}}$, i.e., the interatomic distance corresponding to the first minimum of the radial distribution function $g(r)$ (Fig. 9). For both temperatures $R_{12_{\max}}=1.35$ was used. At the higher temperature nearly totally ordered clusters are formed with $\langle F_o \rangle = 96\%$, while clusters formed at the lower temperature are rather highly disordered ($\langle F_o \rangle = 53\%$). This means that an increase in temperature enables the reconstruction of atom arrangement within a cluster. It may be attributed to an easier passing through the free energy barriers at the higher temperature, which leads to the formation of more ordered structure, i.e., with completed first shell of nearest neighbors and a regular local arrangement of atoms. Problems with attaining sufficiently high bonded and ordered clusters at $T^*=0.05$ were decisive to concentrate our efforts on detailed analysis of spatial location of the structure centers in clusters of higher temperature.

The quantitative dominance of hcp and pdp local arrangement over fcc and icosahedral structural units can be explained for many clusters to be caused by the existence of ic center/centers in the cluster. The role of ic center can be compared with its impact on the internal structure observed in MIC clusters (see Fig. 3), where one ic center always leads to many hcp and pdp centers, and in larger MIC clusters (min. $N=309$) also to many fcc centers. However, most of the obtained clusters are polyicosahedral, with not only one but a few ic structural units, usually well separated one from another by one interatomic distance. A typical picture of such cluster structure is shown in Fig. 10. Interpenetrating or sticking ic structural units appear rarely. Figure 11 shows typical arrangement of ic centers in different clusters, where the triangular and tetrahedral forms are most common ic arrangements in the clusters. Even clusters with more than four

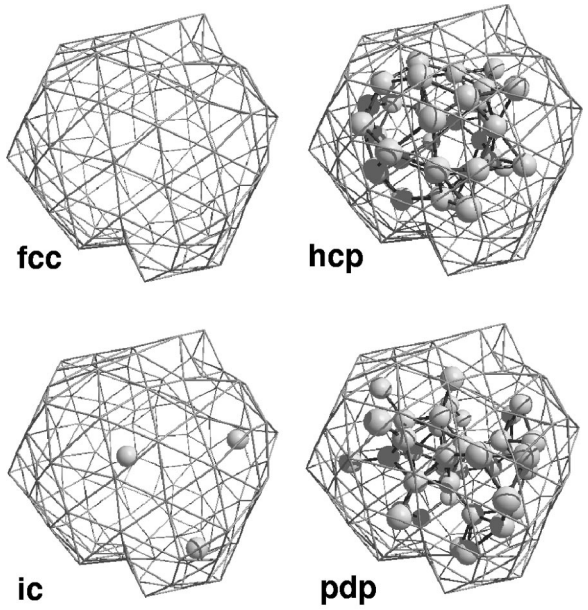

FIG. 10. Common picture of internal structure of clusters formed at $T^*=0.25$: dominance of interpenetrating itself hcp and pdp local structures, absence of fcc and presence of some, here three, ic structural units.

ic centers have some of them arranged in one or both of the ic neighborhood type [see Fig. 11(e)].

In the vast majority of the clusters formed the fcc structure is absent. However, there are clusters where fcc centers are numerous, sometimes fcc dominates in a cluster. One of such clusters is presented in Fig. 12. In this case, the fcc phase is in the form of a plane coming through the cluster center. Two ic units lie on the cluster surface far apart from the fcc region. Spatial separation of ic and fcc structures is also characteristic for others clusters. To a lesser extent, this is true for fcc and pdp. On the contrary, fcc and hcp centers often are neighboring atoms, thus forming phases which interpenetrate each another. A different type of fcc existence is shown in Fig. 13, which displays two clusters possessing only fcc and hcp type of local order. The absence of noncrystallographic ic and pdp atom arrangement results here in the formation of nice atomic planes in the entire cluster. This also results in the evident spatial separation of both phases in the form of fcc and hcp domains [Fig. 13(a)] or in sandwiched parallel fcc and hcp planes [Fig. 13(b)]. Both of these phases are in thermal equilibrium, therefore, the number of structural units fluctuates around an average value. The phase shape is observed to change slightly, yet none of the two phases disappears in the course of the simulation.

V. CONCLUSIONS

The analysis of the shape of a coordination polyhedron, enabled by the algorithm presented in this work, proves to be a proper method for the detection of five types of local structures (fcc, hcp, ic, pdp, and bcc) in finite clusters. The coordination polyhedron method, when accompanied by the visualization used here, gives us a powerful tool for the analysis of local structures existing not only in clusters but

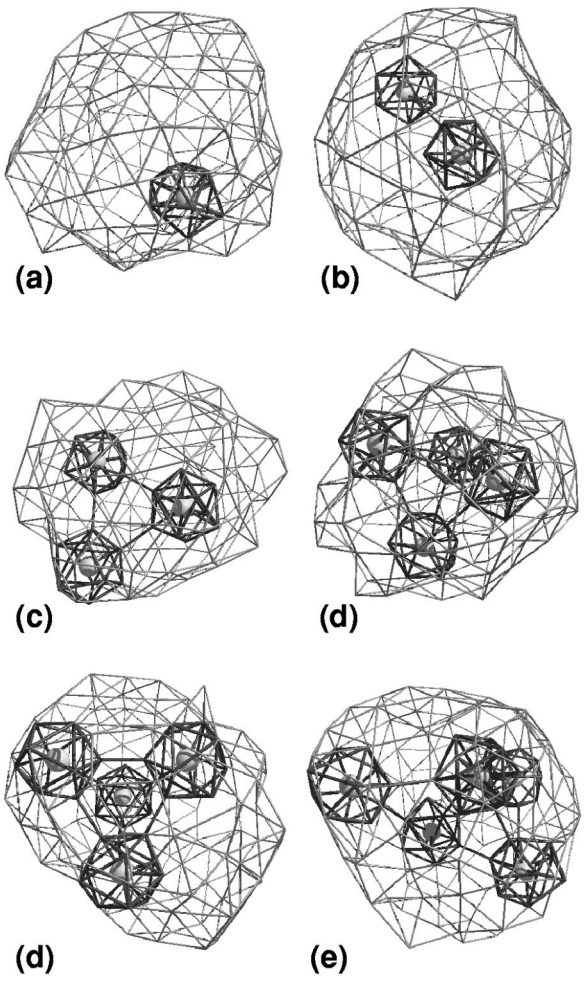

FIG. 11. Examples of spatial arrangement of (a) one, (b) two, (c) three (triangular form), (d) four (tetrahedral form), and (e) five ic centers in clusters at $T^*=0.25$.

also in bulk solids and liquids. Recently, the CP method has been successfully applied to observe structural transition from noncrystalline ic ordering in small clusters to a mixture of fcc and hcp layers during simulated growth of LJ clusters.[37]

The initially perfect (at $T^*=0$) clusters of three types of atom arrangement: fcc, hcp, and bcc, show structural transition during the heating. This transition always occurs by the formation of some centers of a new local structure in the temperature range corresponding to the solid clusters, i.e., before cluster melting. In our opinion, this transition can lead to more optimal cluster structure characterized by the lower value of the free energy F probably due to an increase in the entropy S in less ordered clusters. Therefore, the results obtained by finding the global minimum of the potential energy U are not valid at sufficiently high temperatures. Calculated from results reported in this paper $T^*=0.29$, the transition temperature $T=35$ K is identical to the cluster temperature estimated from the experimental data $T=35\pm4$ K.[5,11] According to Refs. 5 and 11 the cluster temperature appears to be size independent. It implies that experimental clusters of size $N\approx200$ cannot have one crystallographic ideal structure

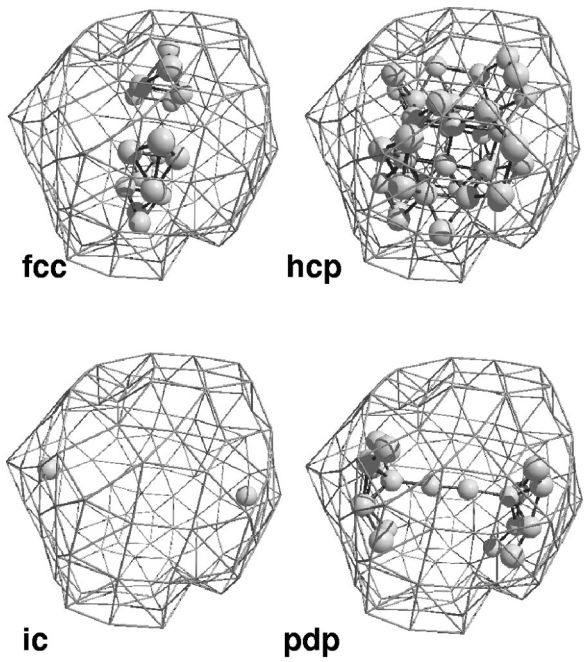

FIG. 12. Coexistence of four types of structural units in a cluster at $T^*=0.25$. Spatial separation of fcc and ic structures, and, to a lesser extend, fcc and pdp is shown.

as a consequence of the natural coexistence of phases at sufficiently high temperatures.

The spectrum of the 201 atom clusters equilibrated at temperature $T^*=0.25$ is characterized by a variety of local structures, with the absence of bcc units. In some cases, four types of structures were found to coexist in the same cluster which is characteristic for larger MIC clusters ($N\geqslant309$).

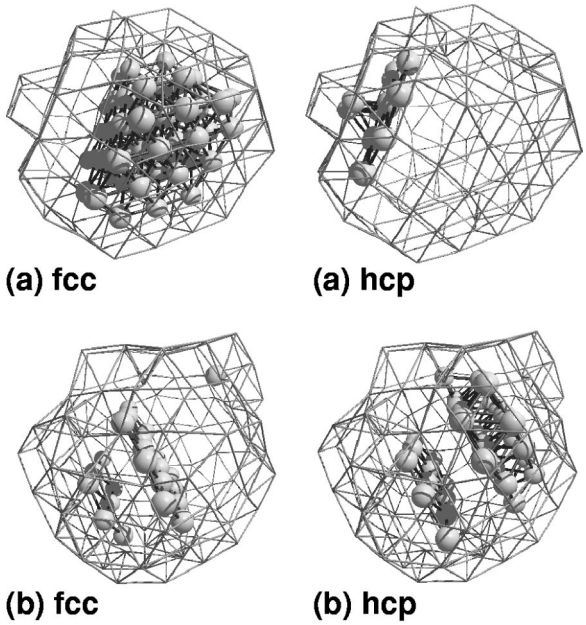

FIG. 13. Two examples of coexistence of only fcc and hcp types of local structures in clusters characterized by (a) two spatially separated fcc and hcp domains, (b) parallel two fcc and three hcp planes.

Most of the other clusters possess only three types of structure: hcp, ic, and pdp, what is typical for smaller MIC clusters with $N=147$ and 55. However, an important difference is that most of them are polyicosahedral, very often showing surprisingly regular triangular or tetrahedral arrangement of ic units.

Visual inspection of clusters with only fcc and hcp structure revealed that the positions of centers of structural units are often ordered in a planelike manner. The role of such highly ordered clusters in cluster growth seems to be of great importance, if their unique structure could be maintained at larger sizes. In such clusters the formation of a screw dislocation which can speed up their growth (to be investigated in our future work) can be considered possible.

Another form of linear defect is the pdp structure oriented along the common axis of pentagonal symmetry. Of course, such linear defects are present in MIC clusters, but what is important, is that this structure can be formed spontaneously (in the absence of ic unit) also during the heating up of an initially perfect cluster [cf. Fig. 7(c)] or during the cluster formation. It should be emphasized that the formation of such local arrangement during the growth of small clusters has been excluded by Hoare and Pal,[15] but dislocations of fivefold axial symmetry have been postulated by van de Waal[21] to exist in large clusters to enable fcc overgrowth.

ACKNOWLEDGMENTS

One of the authors (W.P.) wishes to thank Dr. K. Grabowski and Dr. T. Zientarski for their helpful assistance during his stay at MCS University, and Professor K. Sangwal for his constant interest in the work. He also gratefully acknowledges the support by Grant No. KBN/SGI_ORIGIN_2000/PLubelska/064/199 from ACK Cyfronet AGH (Cracow, Poland) giving him an opportunity to make simulations on the computer SGI2000. A.P. thanks KBN (Poland) for financial support under Grant No. 3 T09A 16118.

[1] C. Kittel, *Introduction to Solid State Physics*, 5th ed. (Wiley, New York, 1976), Chap. 3.
[2] F.H. Stillinger, J. Chem. Phys. **115**, 5208 (2001).
[3] K.F. Niebel and J.A. Venables, ''The crystal structure problem,'' in *Rare Gas Solids*, edited by M.L. Klein and J.A. Venables (Academic, London, 1976), Chap. 9.
[4] T. Ikeshoji, G. Torchet, M.-F. de Feraudy, and K. Koga, Phys. Rev. E **63**, 031101 (2001).
[5] B.W. van de Waal, G. Torchet, and M.-F. de Feraudy, Chem. Phys. Lett. **331**, 57 (2000).
[6] S. Sugano, *Microcluster Physics* (Springer-Verlag, Berlin Heidelberg, 1991).
[7] H. Haberland, ''Rare gas clusters,'' in *Clusters of Atoms and Molecules I*, edited by H. Haberland (Springer, Berlin, 1995), Chap. 4.6.
[8] J. Farges, B. Raoult, and G. Torchet, J. Chem. Phys. **59**, 3454 (1973).
[9] B.W. van de Waal, Phys. Rev. Lett. **76**, 1083 (1996).
[10] S.I. Kovalenko, D.D. Solnyshkin, E.T. Verkhovtseva, and V.V. Eremenko, Chem. Phys. Lett. **250**, 309 (1996).
[11] M.-F. de Feraudy and G. Torchet, J. Cryst. Growth **217**, 449 (2000).
[12] M.R. Hoare and P. Pal, Adv. Phys. **20**, 161 (1971).
[13] J.P.K. Doye, D.J. Wales, and R.S. Berry, J. Chem. Phys. **103**, 4234 (1995).
[14] J.P.K. Doye and F. Calvo, Phys. Rev. Lett. **86**, 3570 (2001).
[15] M.R. Hoare and P. Pal, J. Cryst. Growth **17**, 77 (1972).
[16] R.S. Berry and B.M. Smirnov, J. Chem. Phys. **113**, 728 (2000).
[17] T. Ikeshoji, B. Hafskjold, Y. Hashi, and Y. Kawazoe, J. Chem. Phys. **105**, 5126 (1996).
[18] J. Farges, M.F. de Feraudy, B. Raoult, and G. Torchet, J. Chem. Phys. **78**, 5067 (1983).
[19] J.P. Neirotti, F. Calvo, D.L. Freeman, and J.D. Doll, J. Chem. Phys. **112**, 10340 (2000).
[20] N. Quirke, Mol. Simul. **1**, 249 (1988).
[21] B.W. van de Waal, J. Cryst. Growth **158**, 153 (1996).
[22] S. Kakar, O. Björneholm, J. Weigelt, A.R.B. de Castro, L. Tröger, R. Frahm, T. Möller, A. Knop, and E. Rühl, Phys. Rev. Lett. **78**, 1675 (1997).
[23] F. Baletto, J.P.K. Doye, and R. Ferrando, Phys. Rev. Lett. **88**, 075503 (2002).
[24] F. Baletto, C. Mottet, and R. Ferrando, Phys. Rev. B **63**, 155408 (2001).
[25] A. Rytkönen, S. Valkealahti, and M. Manninen, J. Chem. Phys. **108**, 5826 (1998).
[26] F. Calvo and P. Labastie, Chem. Phys. Lett. **258**, 233 (1996).
[27] R. Mahnke, H. Urbschat, and A. Budde, Z. Phys. D: At., Mol. Clusters **20**, 399 (1991).
[28] P.J. Steinhardt, D.R. Nelson, and M. Ronchetti, Phys. Rev. B **28**, 784 (1983).
[29] H. Gades and A.C. Mitus, Physica A **176**, 297 (1991).
[30] A.C. Mitus, F. Smolej, H. Hahn, and A.Z. Patashinski, Europhys. Lett. **32**, 777 (1995).
[31] J.P.K. Doye, M.A. Miller, and D.J. Wales, J. Chem. Phys. **110**, 6896 (1999).
[32] R. Laskowski, J. Rybicki, and M. Chybicki, T.A.S.K. Quarterly (Poland) **1**, 96 (1997).
[33] W. Brostow, M. Chybicki, R. Laskowski, and J. Rybicki, Phys. Rev. B **57**, 13 448 (1998).
[34] Y. Fukano and C.M. Wayman, J. Appl. Phys. **40**, 1656 (1969).
[35] H. Vehkamäki and I.J. Ford, J. Chem. Phys. **112**, 4193 (2000).
[36] C.L. Cleveland, W.D. Luedtke, and U. Landman, Phys. Rev. Lett. **81**, 2036 (1998).
[37] W. Polak (unpublished).